

# Three-pion exchange nucleon-nucleon potentials with virtual $\Delta$ -isobar excitation<sup>1</sup>

N. Kaiser

Physik-Department T39, Technische Universität München, D-85747 Garching, Germany

## Abstract

The nucleon-nucleon interaction arising from the exchange of three pions and the excitation of  $\Delta(1232)$ -isobars in intermediate states is studied. Approximating the  $\Delta$ -propagator by the inverse  $\Delta N$  mass-splitting, analytical expressions are derived for the spectral-functions of the isoscalar and isovector central, spin-spin and tensor NN-potentials in momentum-space. A translation of the spectral-functions into coordinate-space potentials reveals that the main effect of these specific exchange and excitation mechanisms is a repulsive isoscalar central NN-potential.

## 1 Introduction and summary

The interaction between two nucleons based on chiral effective field theory has been studied in great detail over the past two decades, for reviews see [1, 2, 3, 4]. Most calculations employ the effective chiral Lagrangian formulated in terms of pions and nucleons that are chirally coupled with each other and to external sources. The excitation of baryon and meson resonances is encoded in the low-energy constants of the chiral pion-nucleon interaction terms of higher order. Such a framework provides an accurate description of the empirical nucleon-nucleon phase shifts, if extended to sufficiently high order. At the present time, calculations have been carried out up to order  $N^4\text{LO}$  in the chiral (low-momentum) expansion [5, 6] and the incorporation of dominant contributions at order  $N^5\text{LO}$  is underway. Still, it can be argued the explicit inclusion the  $\Delta(1232)$ -isobar, the most prominent resonance in nuclear physics, allows one to resum a certain class of important contributions and therefore may lead to an improved convergence. In such a phenomenological extension of baryon chiral perturbation theory the delta-nucleon mass splitting,  $\Delta = 293\text{ MeV}$ , is counted as an additional small scale parameter, comparable to the typical momentum  $p$  or the pion mass  $m_\pi$ . The finite-range parts of the  $2\pi$ -exchange NN-interaction as generated by the pertinent triangle and box diagrams with intermediate  $\Delta(1232)$ -isobars have been calculated first in ref. [7] using the Feynman diagram technique. Furthermore, the Bochum-Bonn group [8, 9] has worked out the subleading isospin-conserving corrections as well as the isospin-breaking corrections provided by the chirally interacting  $\pi N\Delta$ -system.

The purpose of the present paper is to analyze the two-nucleon interaction which arises from the exchange of three pions in combination with excitations of  $\Delta(1232)$ -isobars in intermediate states. In this sense it represents an extension of earlier works on the  $3\pi$ -exchange NN-interaction in refs. [10, 11] to chiral effective field theory with explicit  $\Delta(1232)$ -isobar degrees of freedom.

The present paper is organized as follows. In section 2, the techniques to calculate spectral-functions (or imaginary parts) of two-loop  $3\pi$ -exchange diagrams in the heavy nucleon mass limit are prepared. In order to facilitate an analytical treatment (of at least the angular part) of the involved  $3\pi$ -phase space integrals, the non-relativistic  $\Delta$ -propagator will be approximated by the inverse mass-splitting  $\Delta^{-1}$ . A consequence of this approximation is that the pion-induced excitation and deexcitation of virtual  $\Delta(1232)$ -isobars can be conveniently condensed into (symmetrized)  $2\pi$ - and  $3\pi$ -contact vertices with a nucleon. In section 3, analytical expressions are derived for the spectral-functions corresponding to the isoscalar and isovector central, spin-spin and tensor NN-potentials in

---

<sup>1</sup>This work has been supported in part by DFG and NSFC (CRC110).

momentum-space. This is separately done for five different classes of  $3\pi$ -exchange diagrams which are grouped together according to the number of intermediate  $\Delta(1232)$ -isobar excitations. For each class the resulting NN-potentials in coordinate-space are displayed in the distance region  $1 \text{ fm} < r < 2 \text{ fm}$ . As a summary one finds that the main effect of these specific exchange and excitation mechanisms is a repulsive isoscalar central NN-potential  $\tilde{V}_C(r)$ . Moreover, the contributions to the isovector tensor potential  $\tilde{W}_T(r)$  tend to cancel each other, while other components come out very small anyway. This overall result is remarkable in view of the fact that previous calculations of the chiral three-pion exchange NN-interaction in refs. [10, 11] have lead to a vanishing isoscalar central potential.

## 2 Preparation

Let us start with recalling the form of the (static) nucleon-nucleon potential in momentum-space:

$$T_{NN} = V_C(q) + V_S(q) \vec{\sigma}_1 \cdot \vec{\sigma}_2 + V_T(q) \vec{\sigma}_1 \cdot \vec{q} \vec{\sigma}_2 \cdot \vec{q} + \{W_C(q) + W_S(q) \vec{\sigma}_1 \cdot \vec{\sigma}_2 + W_T(q) \vec{\sigma}_1 \cdot \vec{q} \vec{\sigma}_2 \cdot \vec{q}\} \vec{\tau}_1 \cdot \vec{\tau}_2, \quad (1)$$

where  $q = |\vec{q}|$  denotes the momentum transfer between the initial- and final-state nucleons. The subscripts  $C, S$  and  $T$  refer to the central, spin-spin and tensor-type components, each of which occurs in an isoscalar ( $V_{C,S,T}$ ) and an isovector version ( $W_{C,S,T}$ ). The sign-convention for  $T_{NN}$  is chosen such that the usual one-pion exchange gives:  $W_T(q)^{(1\pi)} = (g_A/2f_\pi)^2(m_\pi^2 + q^2)^{-1}$ . The occurring physical parameters are: the nucleon axial-vector coupling constant  $g_A = 1.29$ , the pion decay constant  $f_\pi = 92.4 \text{ MeV}$ , and the average pion mass  $m_\pi = 138 \text{ MeV}$ .

We are interested in the finite-range parts of  $T_{NN}$  that are generated by certain  $3\pi$ -exchange diagrams. For this purpose it is sufficient to calculate the imaginary parts  $\text{Im}V_{C,S,T}(i\mu)$  and  $\text{Im}W_{C,S,T}(i\mu)$ , obtained by analytical continuation to time-like momentum transfer  $q = i\mu$ , with  $\mu > 3m_\pi$ . These imaginary parts serve also as the mass spectra entering a representation of the (local) coordinate-space potentials in the form of a continuous superposition of Yukawa functions:

$$\tilde{V}_C(r) = -\frac{1}{2\pi^2 r} \int_{3m_\pi}^{\Lambda} d\mu \mu e^{-\mu r} \text{Im}V_C(i\mu), \quad (2)$$

$$\tilde{V}_S(r) = \frac{1}{6\pi^2 r} \int_{3m_\pi}^{\Lambda} d\mu \mu e^{-\mu r} [\mu^2 \text{Im}V_T(i\mu) - 3\text{Im}V_S(i\mu)], \quad (3)$$

$$\tilde{V}_T(r) = \frac{1}{6\pi^2 r^3} \int_{3m_\pi}^{\Lambda} d\mu \mu e^{-\mu r} (3 + 3\mu r + \mu^2 r^2) \text{Im}V_T(i\mu) \quad (4)$$

with  $\Lambda$  the spectral cutoff, set to a maximal value of  $\Lambda = 1.5 \text{ GeV}$  in ref. [5]. For the isovector potentials  $\tilde{W}_{C,S,T}(r)$  a completely analogous representation holds. Note that the tensor potentials  $\tilde{V}_T(r)$  and  $\tilde{W}_T(r)$  are accompanied by the usual tensor operator  $3\vec{\sigma}_1 \cdot \hat{r} \vec{\sigma}_2 \cdot \hat{r} - \vec{\sigma}_1 \cdot \vec{\sigma}_2$ .

Making use of the Cutkosky cutting rules, the imaginary parts entering eqs.(2,3,4) are calculated from the pertinent two-loop  $3\pi$ -exchange diagrams as integrals of the  $\bar{N}N \rightarrow 3\pi \rightarrow \bar{N}N$  transition amplitudes over the Lorentz-invariant three-pion phase-space. In the center-of-mass frame this four-dimensional phase-space integral includes an angular part of the form:

$$\iint_E \frac{dx dy}{\sqrt{1 - x^2 - y^2 - z^2 + 2xyz}} \cdots, \quad (5)$$

with  $x = \vec{v} \cdot \hat{k}_1$  and  $y = \vec{v} \cdot \hat{k}_2$  the directional cosines of two pion-momenta  $\vec{k}_{1,2}$ . The unit-vector  $\vec{v}$  is introduced by the four-velocity  $v^\alpha = (0, i\vec{v})$  of the heavy nucleon in the considered  $t$ -channel

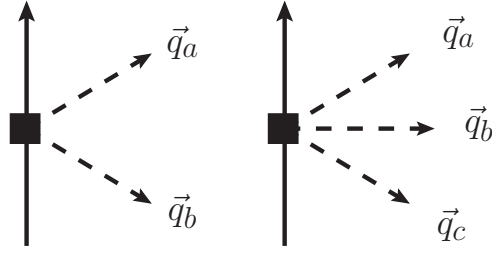


Figure 1: Contact-vertices of two and three pions with a nucleon arising from the excitation of intermediate  $\Delta(1232)$ -isobars.

kinematics  $\bar{N}N \rightarrow 3\pi \rightarrow \bar{N}N$  [10]. The integration region  $E$  in eq.(5) is an ellipse  $x^2 + y^2 - 2xyz < 1 - z^2$  with semi-axes  $\sqrt{1+z}$  and  $\sqrt{1-z}$ , where  $z = \hat{k}_1 \cdot \hat{k}_2$  (see also eq.(28)). In order to allow for an analytical treatment of the angular integral in eq.(5) for all two-loop  $3\pi$ -exchange diagrams, we approximate the non-relativistic delta-propagator by the inverse delta-nucleon mass splitting  $\Delta^{-1}$ . In the case of a simple one-loop  $2\pi$ -exchange triangle diagram this approximation leads to the inequality:

$$\frac{\sqrt{\mu^2 - 4m_\pi^2}}{\mu\Delta} > \frac{2}{\mu} \arctan \frac{\sqrt{\mu^2 - 4m_\pi^2}}{2\Delta}, \quad (6)$$

where the complete result stands on the right hand side. A comparison of the associated central potentials reveals that the approximation using  $\Delta^{-1}$  leads to an overestimation by about 10 – 20%. Although the kinematical situation is more complex for  $3\pi$ -exchange, one can expect that the approximation using  $\Delta^{-1}$  provides an upper bound for the NN-potentials with a similar error margin.

Once the energy-dependence of the delta-propagator is neglected, one can combine the direct and crossed  $\Delta(1232)$ -isobar excitation to a  $2\pi$ -contact vertex as symbolized by a filled square in the left diagram of Fig. 1. The corresponding transition matrix-element reads:

$$M_{2\pi\Delta} = \frac{ig_A^2}{4f_\pi^2\Delta} \left\{ \epsilon_{abc}\tau_c \vec{\sigma} \cdot (\vec{q}_a \times \vec{q}_b) - 4\delta_{ab} \vec{q}_a \cdot \vec{q}_b \right\}, \quad (7)$$

where  $\vec{q}_a$  and  $\vec{q}_b$  denote both outgoing pion-momenta. In order to arrive at this form the relation  $T_a T_b^\dagger = (2\delta_{ab} - i\epsilon_{abc}\tau_c)/3$  for the isospin (and spin) transition operators and the coupling constant ratio  $g_{\pi N\Delta}/g_{\pi NN} = 3/\sqrt{2}$  have been used. The strong  $\pi NN$ -coupling constant follows from the Goldberger-Treiman relation as  $g_{\pi NN} = g_A M/f_\pi = 13.1$ , with  $M = 939$  MeV the nucleon mass. The delta-nucleon mass splitting  $\Delta$  has the well-known value  $\Delta = 293$  MeV.

Fig. 1 shows on the right also a diagram with a  $3\pi$ -contact vertex which arises from an additional direct coupling of the pion to the  $\Delta(1232)$ -isobar. Summing over the six permutations of the isospin-indices  $(a, b, c)$  the corresponding transition matrix-element reads:

$$M_{3\pi\Delta\Delta} = \frac{g_A^3}{40f_\pi^3\Delta^2} \left\{ -75\epsilon_{abc} \vec{q}_a \cdot (\vec{q}_b \times \vec{q}_c) + \vec{q}_a \cdot \vec{q}_b \vec{\sigma} \cdot \vec{q}_c (18\delta_{ab}\tau_c - 7\delta_{ac}\tau_b - 7\delta_{bc}\tau_a) \right. \\ \left. + \vec{q}_a \cdot \vec{q}_c \vec{\sigma} \cdot \vec{q}_b (18\delta_{ac}\tau_b - 7\delta_{ab}\tau_c - 7\delta_{bc}\tau_a) + \vec{q}_b \cdot \vec{q}_c \vec{\sigma} \cdot \vec{q}_a (18\delta_{bc}\tau_a - 7\delta_{ac}\tau_b - 7\delta_{ab}\tau_c) \right\}, \quad (8)$$

where  $\vec{q}_a, \vec{q}_b, \vec{q}_c$  denote outgoing pion-momenta. In order to fix the  $\Delta\Delta\pi$ -vertex we use the coupling constant ratio  $g_{\pi\Delta\Delta}/g_{\pi NN} = 1/5$  of the quark-model. Furthermore, the relation for the isospin (transition) operators,  $T_a \Theta_b T_c^\dagger = (5i\epsilon_{abc} - \delta_{ab}\tau_c + 4\delta_{ac}\tau_b - \delta_{bc}\tau_a)/3$ , with  $\Theta_b$  the  $4 \times 4$   $\Delta$ -isospin matrices, has been employed together with an analogous relation for the spin (transition) operators.

While the decomposition into isoscalar and isovector contributions is obvious from the isospin factor  $V + W \vec{\tau}_1 \cdot \vec{\tau}_2$  of a  $3\pi$ -exchange diagram, a certain technique is needed in order to separate the

spin-spin and tensor-like components. First, one removes from a spin-dependent expression of the form  $\vec{\sigma}_1 \cdot \vec{A} \vec{\sigma}_2 \cdot \vec{B}$  the Pauli-matrices  $\vec{\sigma}_1$  and  $\vec{\sigma}_2$ . The spin-spin part  $\text{Im}V_S$  is then obtained by contracting the Lorentz-tensor  $A_\alpha B_\beta$  with the projector  $\frac{1}{2}(v^\alpha v^\beta + \mu^{-2} q^\alpha q^\beta - g^{\alpha\beta})$ , and the combination  $\text{Im}(\mu^2 V_T - V_S)$  including the tensor part follows finally by contracting  $A_\alpha B_\beta$  with the projector  $\mu^{-2} q^\alpha q^\beta$ . After these manipulations the relevant expressions are given in terms of Lorentz-scalars, which can be easily translated from the  $s$ -channel ( $NN \rightarrow NN$ ) into the  $t$ -channel ( $\bar{N}N \rightarrow 3\pi \rightarrow \bar{N}N$ ).

### 3 Calculation of spectral functions and r-space potentials

In this section, we present the analytical expressions for the spectral-functions pertaining to the isoscalar and isovector central, spin-spin and tensor NN-potentials in momentum-space. This is done separately in five subsections for the different classes of  $3\pi$ -exchange diagrams, ordered according to the number of intermediate  $\Delta(1232)$ -isobar excitations. In all cases the technical details are omitted and only the final results for the non-vanishing contributions are given. The calculated spectral-functions are then used to construct the corresponding NN-potentials in coordinate-space. These are presented in five figures displaying their dependence on the distance  $r$  in the region  $1 \text{ fm} < r < 2 \text{ fm}$ .

#### 3.1 Single $\Delta$ -excitation of one nucleon

We start with the  $3\pi$ -exchange diagrams with a single  $\Delta(1232)$ -excitation of one nucleon. The corresponding diagrams are compiled in ref. [11], where they have been grouped into the classes X, XI, XII, XIII and XIV. The subleading  $2\pi$ -contact vertex treated in ref. [11] includes  $M_{2\pi\Delta}$  as a special case, namely by setting the low-energy constants to the values:  $c_1 = 0$ ,  $c_2 = -c_3 = 2c_4 = g_A^2/2\Delta$ . Therefore, it suffices to evaluate the  $dw$ -integrals in eqs.(7-22) of ref. [11] for these parameter values. It is convenient to introduce the dimensionless variable  $u = \mu/m_\pi > 3$  and the auxiliary functions:

$$R(u) = (u-1)\sqrt{(u-3)(u+1)}, \quad L(u) = \ln \frac{\sqrt{u-3} + \sqrt{u+1}}{2}. \quad (9)$$

The contributions proportional to  $g_A^4$  which arise from the classes X, XI and XII read:

$$\text{Im}V_S = \frac{g_A^4 m_\pi^5}{(4f_\pi)^6 \pi^2 \Delta} \left\{ \frac{R(u)}{48} \left[ 100 - \frac{27}{u^3} - \frac{50}{u^2} - \frac{151}{u} + 185u - 14u^2 - 7u^3 \right] + 2L(u) \left[ \frac{2}{u^3} + \frac{10}{u} - 9u \right] \right\}, \quad (10)$$

$$\text{Im}(\mu^2 V_T - V_S) = \frac{g_A^4 m_\pi^5}{(4f_\pi)^6 \pi^2 \Delta} \left\{ \frac{R(u)}{24} \left[ u^3 + 2u^2 - 39u - 12 + \frac{65}{u} - \frac{50}{u^2} - \frac{27}{u^3} \right] + 4L(u) \left[ \frac{2}{u^3} - \frac{10}{u} + 3u \right] \right\}, \quad (11)$$

$$\text{Im}W_S = \frac{g_A^4 m_\pi^5}{(4f_\pi)^6 \pi^2 \Delta} \left\{ \frac{R(u)}{72} \left[ \frac{135}{u^3} + \frac{58}{u^2} - \frac{277}{u} - 36 + 147u - 10u^2 - 5u^3 \right] + 4L(u) \left[ \frac{2}{3u^3} + \frac{2}{3u} - u \right] \right\}, \quad (12)$$

$$\begin{aligned} \text{Im}(\mu^2 W_T - W_S) = & \frac{g_A^4 m_\pi^5}{(4f_\pi)^6 \pi^2 \Delta} \left\{ R(u) \left[ \frac{15}{4u^3} + \frac{29}{18u^2} + \frac{77}{9u} - \frac{13}{2} - \frac{u}{4} + \frac{2u^2}{9} + \frac{u^3}{9} \right. \right. \\ & \left. \left. - \frac{1}{2(u+1)} - \frac{29}{6(u-1)} \right] + 8L(u) \left[ \frac{2}{3u^3} + \frac{11}{3u} + \frac{u}{u^2-1} \right] \right\}. \end{aligned} \quad (13)$$

The additional contributions proportional to  $g_A^6$  from the classes XIII and XIV take the form:

$$\text{Im}W_C = \frac{g_A^6 m_\pi^5}{(4f_\pi)^6 \pi^2 \Delta} \left\{ \frac{2R(u)}{3} [u - 2u^2 - u^3 - 4] + 16L(u) \left[ \frac{1}{u} - 4u + u^3 \right] \right\}, \quad (14)$$

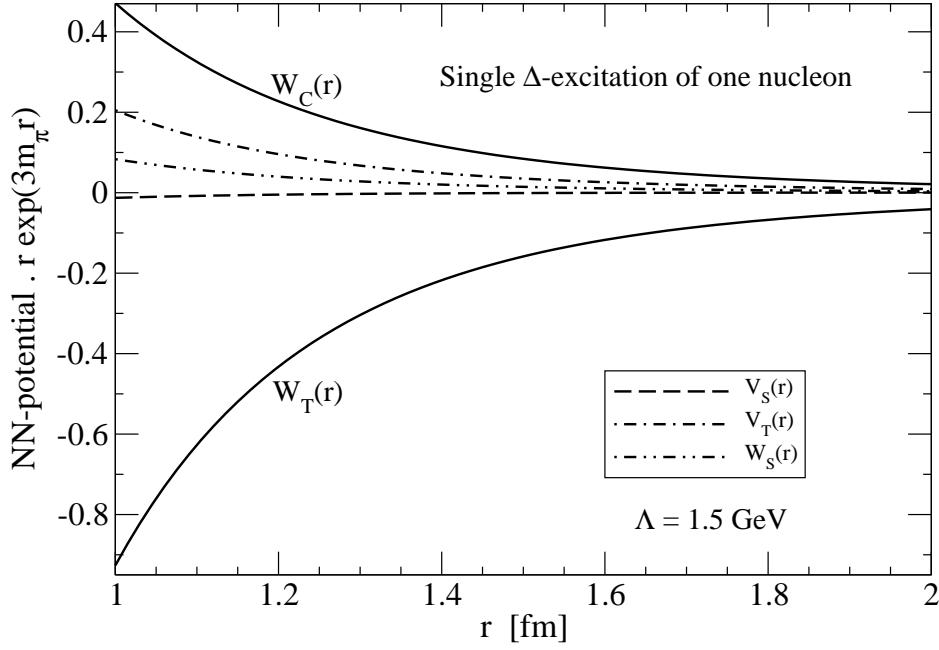


Figure 2: NN-potentials arising from  $3\pi$ -exchange with single  $\Delta$ -excitation of one nucleon.

$$\text{Im}V_S = \frac{g_A^6 m_\pi^5}{(4f_\pi)^6 \pi^2 \Delta} \left\{ \frac{R(u)}{48} \left[ 13u^3 + 26u^2 - 371u - 76 + \frac{493}{u} - \frac{58}{u^2} - \frac{135}{u^3} \right] + 2L(u) \left[ 15u - \frac{22}{u} - \frac{2}{u^3} \right] \right\}, \quad (15)$$

$$\text{Im}(\mu^2 V_T - V_S) = \frac{g_A^6 m_\pi^5}{(4f_\pi)^6 \pi^2 \Delta} \left\{ \frac{R(u)}{24} \left[ 5u^3 + 10u^2 - 3u - 252 - \frac{443}{u} - \frac{58}{u^2} - \frac{135}{u^3} \right] + 4L(u) \left[ 3u + \frac{22}{u} - \frac{2}{u^3} \right] \right\}, \quad (16)$$

$$\begin{aligned} \text{Im}W_S = & \frac{g_A^6 m_\pi^5}{(4f_\pi)^6 \pi^2 \Delta} \left\{ \frac{R(u)}{144} \left[ 284 - \frac{189}{u^3} - \frac{158}{u^2} - \frac{1249}{u} + 1543u - 210u^2 - 105u^3 \right] \right. \\ & \left. + 2L(u) \left[ \frac{2}{3u^3} + \frac{12}{u} - 17u + 2u^3 \right] \right\}, \end{aligned} \quad (17)$$

$$\begin{aligned} \text{Im}(\mu^2 W_T - W_S) = & \frac{g_A^6 m_\pi^5}{(4f_\pi)^6 \pi^2 \Delta} \left\{ \frac{R(u)}{72} \left[ 972 - \frac{189}{u^3} - \frac{158}{u^2} + \frac{119}{u} + 1503u - 178u^2 - 89u^3 \right] \right. \\ & \left. + 4L(u) \left[ \frac{2}{3u^3} - \frac{22}{3u} - 13u \right] \right\}. \end{aligned} \quad (18)$$

As indicated by the prefactor  $m_\pi^5/\Delta$  all the terms in eqs.(10-18) are of fourth power in small momenta. Thus they are counted of order  $N^3\text{LO}$  in the chiral effective field theory with explicit  $\Delta(1232)$ -isobars. Note also that the isoscalar central component  $\text{Im}V_C$  vanishes identically due to the exact cancellation of the contributions from class XIII and XIV (see eq.(18) in ref. [11]).

The resulting local NN-potentials in coordinate-space are displayed by Fig.2 in the distance region  $1\text{ fm} < r < 2\text{ fm}$ . In order to obtain curves with less rapid decrease in  $r$ , we have divided out a Yukawa function  $\exp(-3m_\pi r)/r$  with the decay-length  $(3m_\pi)^{-1} = 0.48\text{ fm}$ . Such an unscaled Yukawa potential has a strength of  $(24.1, 5.65, 1.49)\text{ MeV}$  at distances  $r = (1.0, 1.5, 2.0)\text{ fm}$ , respectively. One observes from Fig.2 that the strongest component is an attractive isovector tensor potential  $\widetilde{W}_T(r)$ , followed by a repulsive isovector central potential  $\widetilde{W}_C(r)$  of about half that magnitude. The spin-spin potentials,  $\widetilde{V}_S(r)$  and  $\widetilde{W}_S(r)$ , turn out to be particularly weak.

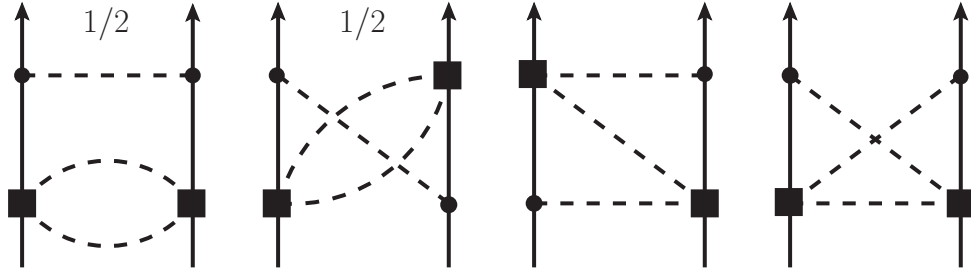


Figure 3: Diagrams related to  $3\pi$ -exchange with single  $\Delta$ -excitation of each nucleon. Upside-down reflected diagrams are not shown. Appropriate symmetry factors  $1/2$  are indicated.

### 3.2 Single $\Delta$ -excitation of both nucleons

Next, we come to the  $3\pi$ -exchange diagrams with a single  $\Delta(1232)$ -excitation of both nucleon. A representative set of two-loop diagrams with pion-bubbles and pions running in zigzag is shown in Fig. 3. The two-nucleon irreducible contributions coming from the planar and crossed bubble diagrams add up to the following results for the spectral-functions:

$$\text{Im}W_C = -\frac{2g_A^6 m_\pi^6}{3\pi^3 (4f_\pi)^6 \Delta^2} \int_2^{u-1} dw (w^2 - 4)^{3/2} \sqrt{\lambda(w)}, \quad (19)$$

$$\begin{aligned} \text{Im}V_S = & \frac{g_A^6 m_\pi^6}{12\pi^3 (4f_\pi)^6 \Delta^2} \int_2^{u-1} dw \frac{(w^2 - 4)^{3/2}}{u^4 \sqrt{\lambda(w)}} \left[ (u^2 - 1)^3 (5u^2 + 1) \right. \\ & \left. + 4w^2 (1 + 2u^2 + 5u^4 - 2u^6) - 2w^4 (3 + 5u^2) + 4(1 + u^2)w^6 - w^8 \right], \end{aligned} \quad (20)$$

$$\text{Im}(\mu^2 V_T - V_S) = \frac{g_A^6 m_\pi^6}{12\pi^3 (4f_\pi)^6 \Delta^2} \int_2^{u-1} dw (w^2 - 4)^{3/2} \sqrt{\lambda(w)} \left[ \frac{2}{u^2} (7w^2 + 1) - \frac{(w^2 - 1)^2}{u^4} - 1 \right], \quad (21)$$

where  $\lambda(w) = w^4 + u^4 + 1 - 2(w^2 u^2 + w^2 + u^2)$  denotes the (kinematical) Källén function. The dimensionless integration variable  $w$  introduced here is the invariant mass of a pion-pair, divided by the pion mass  $m_\pi$ .

The other diagrams in Fig. 3 with pions running in zigzag lead to contributions to the spectral-function which can be given in closed analytical form:

$$\text{Im}V_C = \frac{g_A^6 m_\pi^6}{35\pi (4f_\pi)^6 \Delta^2} (u - 3)^3 \left[ \frac{3}{u} + 3 - 12u - 9u^2 - u^3 \right], \quad (22)$$

$$\text{Im}W_S = \frac{g_A^6 m_\pi^6 (u - 3)^2}{70\pi (4f_\pi)^6 \Delta^2} \left[ 2u^4 + 12u^3 - 21u^2 - \frac{83u}{2} + 80 + \frac{150}{u} - \frac{125}{3u^2} - \frac{125}{2u^3} \right], \quad (23)$$

$$\text{Im}(\mu^2 W_T - W_S) = \frac{g_A^6 m_\pi^6 (u - 3)}{70\pi (4f_\pi)^6 \Delta^2} \left[ \frac{11u^5}{3} + 11u^4 + 2u^3 - 169u^2 + 88u + 33 + \frac{962}{3u} + \frac{125}{u^2} + \frac{375}{u^3} \right], \quad (24)$$

and further contributions which can only be reduced to double-integrals of the form:

$$\text{Im}W_C = -\frac{g_A^6 m_\pi^6 u^2}{(8\pi f_\pi^2)^3 \Delta^2} \iint_{z^2 < 1} d\omega_1 d\omega_2 k_1 k_2 \sqrt{1 - z^2} \arcsin(z), \quad (25)$$

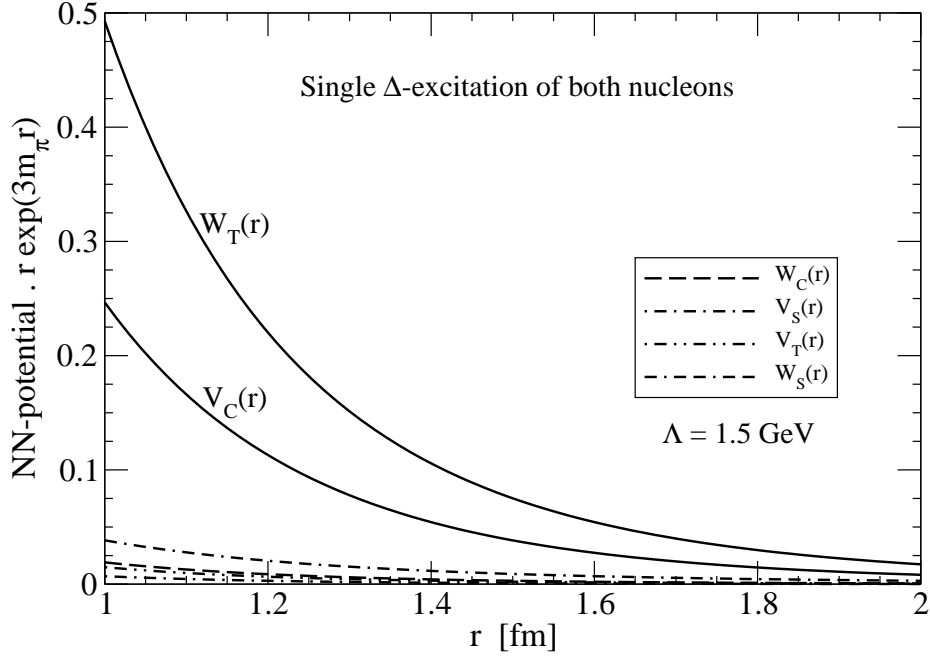


Figure 4: NN-potentials arising from 3 $\pi$ -exchange with single  $\Delta$ -excitation of both nucleons.

$$\begin{aligned}
\text{Im}V_S = & \frac{g_A^6 m_\pi^6}{(8\pi f_\pi^2)^3 \Delta^2} \iint_{z^2 < 1} d\omega_1 d\omega_2 \left\{ \omega_1^2 (9\omega_2 u - \omega_2^2 - 9u^2 - 1) + \frac{3\omega_1}{2} [6u + 6u^3 - \omega_2(1 + 8u^2)] \right. \\
& - \frac{1}{8} (9u^4 + 18u^2 + 5) + \frac{zk_2}{k_1} \left[ \omega_1^3 (\omega_2 - 4u) + \omega_1^2 (2 + 2u^2 - 7\omega_2 u) + 2\omega_1 (2u + \omega_2) \right. \\
& \left. \left. - 2 - 2u^2 + 4\omega_2 u \right] + \frac{3 \arcsin(z)}{k_1 k_2 \sqrt{1 - z^2}} \left[ \omega_1^3 u (2\omega_2 u - u^2 - 1) + \frac{\omega_1^2}{2} (5\omega_2^2 u^2 - \omega_2 u (7 + 11u^2) \right. \right. \\
& \left. \left. + 1 + 4u^2 + 3u^4) + \frac{\omega_1}{8} (\omega_2 (5 + 16u^2 + 15u^4) + 2u - 12u^3 - 6u^5) + \frac{(u^4 - 1)(u^2 + 3)}{16} \right] \right\}, \quad (26)
\end{aligned}$$

$$\begin{aligned}
\text{Im}(\mu^2 V_T - V_S) = & \frac{g_A^6 m_\pi^6}{(8\pi f_\pi^2)^3 \Delta^2} \iint_{z^2 < 1} d\omega_1 d\omega_2 \left\{ 2\omega_1^2 (10\omega_2 u - \omega_2^2 - 6u^2 - 2) - 3u^2 (1 + u^2) \right. \\
& + \omega_1 [10u + 18u^3 - 3\omega_2 (1 + 7u^2)] + \frac{zk_2}{k_1} \left[ \omega_1^3 (2\omega_2 - 7u) - u^2 + \omega_2 u \right. \\
& + \omega_1^2 (3 + 10u^2 - 13\omega_2 u) + \omega_1 (2 + 3u^2) (2\omega_2 - u) \left. \right] + \frac{3 \arcsin(z)}{k_1 k_2 \sqrt{1 - z^2}} \\
& \times (u^2 - 2\omega_1 u + 1) (u^2 - 2\omega_2 u + 1) \left[ \frac{u^2}{4} + \omega_1^2 + \frac{\omega_1}{4} (5\omega_2 - 6u) \right] \left. \right\}. \quad (27)
\end{aligned}$$

The magnitudes of the pion-momenta  $\vec{k}_{1,2}$ , divided by  $m_\pi$ , and their scalar-product are given by:

$$k_1 = \sqrt{\omega_1^2 - 1}, \quad k_2 = \sqrt{\omega_2^2 - 1}, \quad z k_1 k_2 = \omega_1 \omega_2 - u(\omega_1 + \omega_2) + \frac{u^2 + 1}{2}, \quad (28)$$

where the last relation follows from energy conservation. The upper and lower limits of the  $\omega_2$ -integration are  $\omega_2^\pm = \frac{1}{2}(u - \omega_1 \pm k_1 \sqrt{u^2 - 2\omega_1 u - 3/\sqrt{u^2 - 2\omega_1 u + 1}})$ , with  $\omega_1$  lying in the interval  $1 < \omega_1 < (u^2 - 3)/2u$ . Note that the non-algebraic result  $\arcsin(z)/\sqrt{1 - z^2}$  from the angular integral in

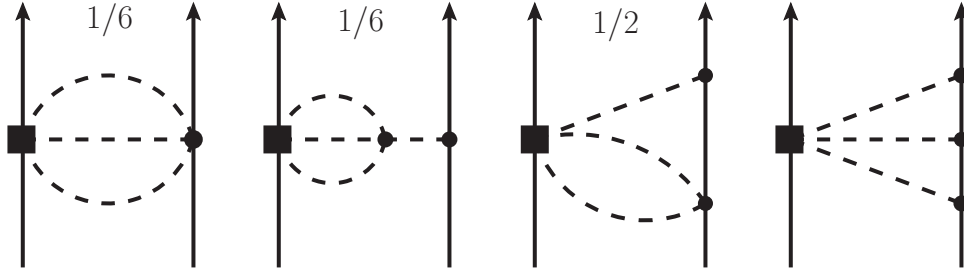


Figure 5: Diagrams related to  $3\pi$ -exchange with double  $\Delta$ -excitation of one nucleon. Left-right reflected diagrams are not shown. Appropriate symmetry factors,  $1/6$  and  $1/2$ , are indicated. The third diagram including a Weinberg-Tomozawa  $2\pi$ -contact vertex vanishes.

eq.(5) prohibits a further step in the analytical integration over the  $3\pi$ -phase space. In the chiral limit  $m_\pi \rightarrow 0$  the double-integrals in eqs.(25,26,27) have the values  $-u^4\pi^2/2520$ ,  $-u^6(\pi^2/7 + 17/24)/360$  and  $u^6(31/24 - \pi^2/7)/720$ , thus these spectral-functions become proportional to  $\mu^6/\Delta^2$ .

Fig.4 shows the resulting NN-potentials in  $r$ -space, multiplied again with  $r \exp(3m_\pi r)$ . One observes as the largest component a repulsive isovector tensor potential  $\widetilde{W}_T(r)$ , and for the first time, a repulsive isoscalar central potential  $\widetilde{V}_C(r)$  of about half that strength. Note that the underlying spectral-functions, written in eqs.(22,23,24) have a rather simple analytical form. Other components of the NN-interaction turn out to be very small for this class of  $3\pi$ -exchange diagrams.

### 3.3 Double $\Delta$ -excitation of one nucleon

Now we consider the diagrams in Fig.5 including (on the left) a double  $\Delta(1232)$ -excitation of one nucleon. The first two diagrams involving the leading order chiral  $3\pi$ -contact vertex and the chiral  $\pi\pi$ -interaction give rise only to isovector spin-dependent contributions (proportional to  $g_A^A$ ) of the form:

$$\begin{aligned} \text{Im}W_S &= \frac{g_A^4 m_\pi^6}{360\pi^3 (4f_\pi u)^6 \Delta^2} \int_2^{u-1} dw \sqrt{w^2 - 4} \lambda^{3/2}(w) \\ &\times \left[ 3 + 78u^2(2 - w^2) + \frac{2}{w^2}(12u^2 - 11u^4 - 1) - w^4 - 11u^4 \right], \end{aligned} \quad (29)$$

$$\begin{aligned} \text{Im}(\mu^2 W_T - W_S) &= \frac{g_A^4 m_\pi^6}{72\pi^3 (4f_\pi u)^6 \Delta^2} \int_2^{u-1} dw \sqrt{(w^2 - 4)\lambda(w)} \left[ u^2 - 3w^2 + 3 + \frac{4(1 - w^2)}{u^2 - 1} \right] \\ &\times \left[ w^4(1 - 43u^2) - w^6 + w^2(u^2 + 3)(47u^2 + 1) \right. \\ &\left. - 3u^6 - 79u^4 - 89u^2 - 5 + \frac{2}{w^2}(u^2 - 1)^2(1 - 3u^2) \right]. \end{aligned} \quad (30)$$

Interestingly, the third diagram in Fig.5 involving the Weinberg-Tomozawa  $2\pi$ -contact vertex leads to vanishing spectral-functions  $\text{Im}W_{S,T} = 0$ . This zero result is not obvious and it is obtained after the third step of the analytical integration over the pion-energy  $\omega_2$ . Hence, one is left with the right diagram in Fig.5 involving three ordinary  $\pi N$ -couplings. The corresponding contributions are proportional to  $g_A^6$  and the double-integral representations of the spectral-functions read:

$$\text{Im}V_C = -\frac{45g_A^6 m_\pi^6 u^2}{2(8\pi f_\pi^2)^3 \Delta^2} \iint_{z^2 < 1} d\omega_1 d\omega_2 k_1 k_2 \sqrt{1 - z^2} \arccos(-z), \quad (31)$$



$$\begin{aligned}
\text{Im}W_S = & \frac{g_A^6 m_\pi^6}{(8\pi f_\pi^2)^3 \Delta^2} \iint_{z^2 < 1} d\omega_1 d\omega_2 \left\{ \frac{\omega_1^3 \omega_2}{3} + \frac{\omega_1^2}{5} (5\omega_2 u - 2\omega_2^2 - 6) - \frac{2}{5} + 2\omega_1 \left[ u + \omega_2 \left( \frac{1}{3} - u^2 \right) \right] \right. \\
& + \frac{zk_2}{6k_1} \left[ \omega_1^3 (9u - 4\omega_2) - \frac{13\omega_1^4}{5} + \frac{\omega_1^2}{5} (9 + 47\omega_2^2 - 60u^2 - 105\omega_2 u) + 5\omega_1 (2\omega_2 + 3u) \right. \\
& + 15\omega_2 u - \frac{56 + 47\omega_2^2}{5} \left. \right] + z^2 (\omega_2^2 - 1) \left[ \frac{3}{5} (2\omega_1^2 + 3) - \omega_1 (\omega_2 + 3u) \right] - \frac{k_1}{3} (zk_2)^3 \\
& + \frac{\arccos(-z)}{k_1 k_2 \sqrt{1-z^2}} \left[ \omega_1^3 u (2\omega_2 u - u^2 - 1) + \omega_1^2 (6u^2 \omega_2^2 - 4\omega_2 (2u^3 + 3u) + u^4 \right. \\
& + \frac{9u^2 + 5}{2}) + \frac{\omega_1}{4} (2\omega_2 (4u^4 + 15u^2 + 5) - u^5 - 16u^3 - 7u) + \frac{u^4 - 5}{4} + u^2 \left. \right] \left. \right\}, \quad (32)
\end{aligned}$$

$$\begin{aligned}
\text{Im}(\mu^2 W_T - W_S) = & \frac{g_A^6 m_\pi^6}{(8\pi f_\pi^2)^3 \Delta^2} \iint_{z^2 < 1} d\omega_1 d\omega_2 \left\{ \frac{2\omega_1}{3} (5u - \omega_1 - \omega_2) (2 + \omega_1 \omega_2) - 4u^2 \omega_1 \omega_2 \right. \\
& + \frac{zk_2}{3k_1} \left[ 5u (3u - \omega_2) + 5\omega_1 (4\omega_2 - u) + \omega_1^2 (12 - 15u^2 - 13\omega_2 u + 6\omega_2^2) \right. \\
& + \omega_1^3 (5u - 2\omega_2) \left. \right] + 2z^2 \omega_1 (\omega_2^2 - 1) (\omega_1 + \omega_2 - 5u) - \frac{(2zk_2)^3 \omega_1^2}{3k_1} \\
& + \frac{\arccos(-z)}{k_1 k_2 \sqrt{1-z^2}} \left[ (1 + u^2) (u - 2\omega_1 - 2\omega_2) + 4\omega_1 \omega_2 u \right] \\
& \times \left[ \frac{3u}{4} (1 + u^2) + \omega_1^2 u + \frac{\omega_1}{2} (6\omega_2 u - 5 - 7u^2) \right] \left. \right\}. \quad (33)
\end{aligned}$$

We note as an aside that in the chiral limit  $m_\pi \rightarrow 0$  the double-integrals in eqs.(31,32,33) have the values  $u^4 \pi^2 / 1260$ ,  $u^6 (\pi^2 - 17/48) / 540$ , and  $u^6 (\pi^2 / 7 + 31/480) / 108$ . Hence, these spectral-functions become again proportional to  $\mu^6 / \Delta^2$ . It should be pointed out that the spin-isospin structure of the  $3\pi$ -contact vertex  $M_{3\pi\Delta\Delta}$  in eq.(8) allows only for an isoscalar central component  $V_C$  and for isovector spin-spin and tensor components  $W_{S,T}$ .

The resulting NN-potentials in  $r$ -space, multiplied with  $r \exp(3m_\pi r)$ , are shown in Fig.6. The dominant feature is now a repulsive isoscalar central potential  $\tilde{V}_C(r)$ , whereas the other potentials  $\tilde{W}_{S,T}(r)$  are suppressed by about one order of magnitude.

### 3.4 Double and single $\Delta$ -excitation of either one nucleon

We continue with the  $3\pi$ -exchange mechanisms accompanied by double and single  $\Delta(1232)$ -excitation of either one nucleon. These are represented by the first two diagrams in Fig.7 (and their mirror partners). In this case the pertinent spectral-functions can be given in closed analytical form and they read:

$$\text{Im}V_C = \frac{5g_A^6 m_\pi^7}{(4f_\pi)^6 \pi^2 \Delta^3} \left\{ \frac{R(u)}{64} \left[ \frac{27}{u} + 50 - 65u + 12u^2 + 39u^3 - 2u^4 - u^5 \right] + 3L(u) \left[ 5u - \frac{3u^3}{2} - \frac{1}{u} \right] \right\}, \quad (34)$$

$$\begin{aligned}
\text{Im}W_S = & \frac{g_A^6 m_\pi^7}{(4f_\pi)^6 \pi^2 \Delta^3} \left\{ \frac{R(u)}{320} \left[ \frac{59u^5}{10} + \frac{59u^4}{5} - \frac{3377u^3}{18} + \frac{4286u^2}{45} + \frac{20057u}{30} \right. \right. \\
& + \frac{307}{3} - \frac{37121}{90u} + \frac{2488}{45u^2} - \frac{372}{5u^3} \left. \right] + L(u) \left[ \frac{u^3}{4} - 5u + \frac{40}{3u} - \frac{59}{30u^3} \right] \left. \right\}, \quad (35)
\end{aligned}$$

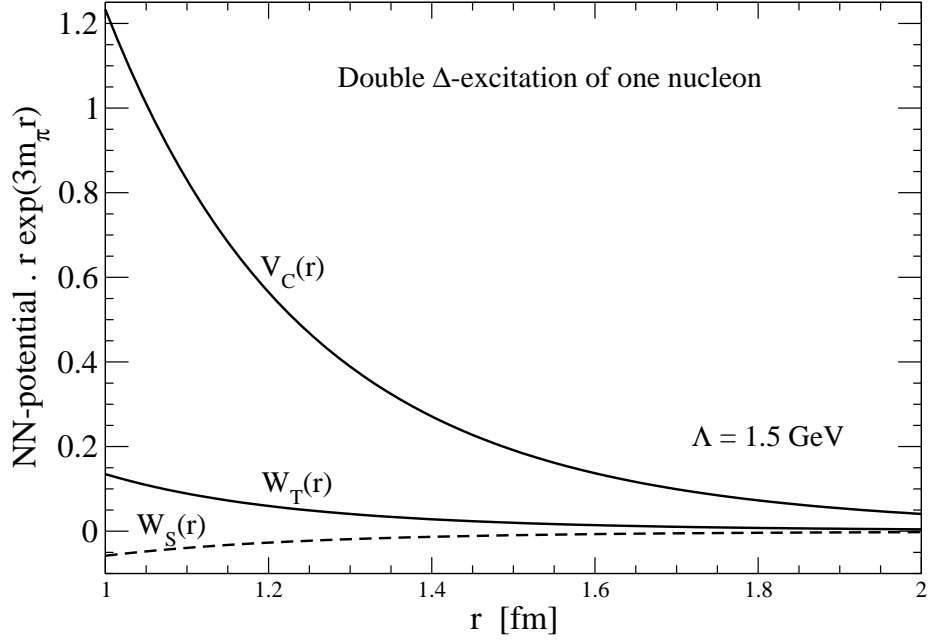


Figure 6: NN-potentials arising from  $3\pi$ -exchange with double  $\Delta$ -excitation of one nucleon.

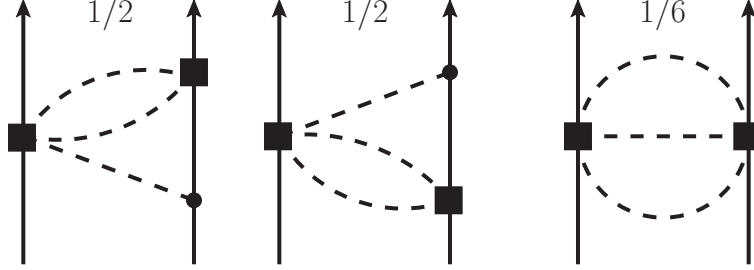


Figure 7: The first two diagrams show  $3\pi$ -exchange with double and single  $\Delta$ -excitation of either one nucleon. The third diagram represents  $3\pi$ -exchange with double  $\Delta$ -excitation of both nucleons. The pertinent symmetry factors,  $1/2$  and  $1/6$ , are indicated.

$$\begin{aligned} \text{Im}(\mu^2 W_T - W_S) = & \frac{g_A^6 m_\pi^7}{(4f_\pi)^6 \pi^2 \Delta^3} \left\{ \frac{R(u)}{120} \left[ \frac{41u^5}{20} + \frac{41u^4}{10} - \frac{305u^3}{12} - \frac{2141u^2}{15} + \frac{5543u}{60} \right. \right. \\ & \left. \left. + \frac{1621}{6} + \frac{29927}{60u} + \frac{622}{15u^2} - \frac{279}{5u^3} \right] + L(u) \left[ 2u^3 - 7u - \frac{41}{3u} - \frac{59}{15u^3} \right] \right\}, \quad (36) \end{aligned}$$

where the auxiliary functions  $R(u)$  and  $L(u)$  have been defined in eq.(9).

The resulting NN-potentials in  $r$ -space, multiplied with  $r \exp(3m_\pi r)$ , are shown in Fig.8. The dominant feature is again a repulsive isoscalar central potential  $\tilde{V}_C(r)$ , while the other potentials  $\tilde{W}_{S,T}(r)$  are suppressed.

### 3.5 Double $\Delta$ -excitation of both nucleons

Finally, there is the  $3\pi$ -exchange mechanism with double  $\Delta(1232)$ -excitation of both nucleons. It is represented by the right diagram in Fig.7. While the imaginary part of the isoscalar central NN-potential  $\text{Im}V_C$  can be given in terms of the short expression:

$$\text{Im}V_C = -\frac{25g_A^6 m_\pi^8}{(4f_\pi)^6 \pi^3 (2\Delta)^4 u^2} \int_2^{u-1} dw [(w^2 - 4)\lambda(w)]^{3/2}, \quad (37)$$

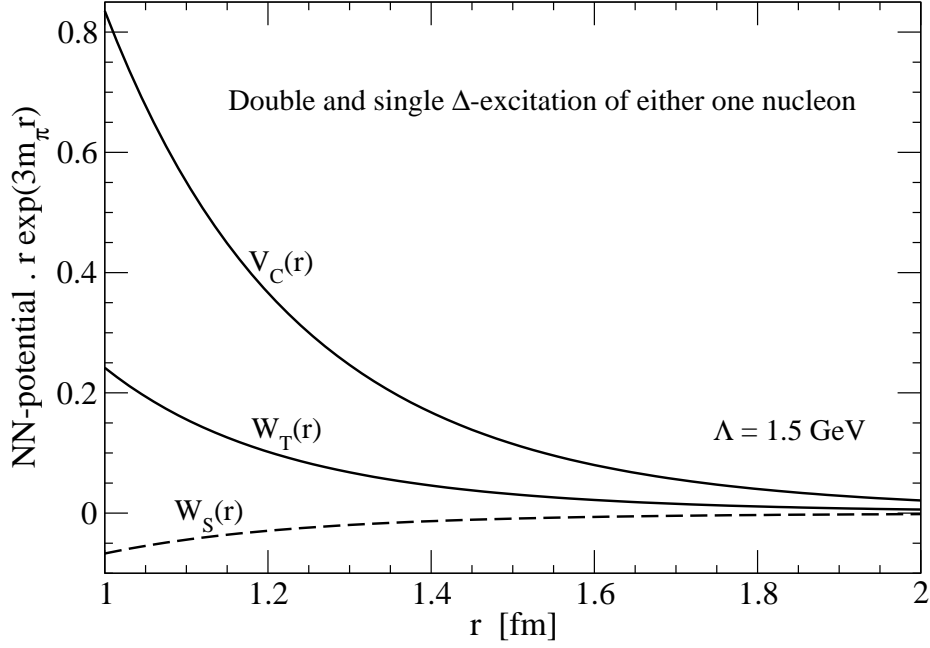


Figure 8: NN-potential arising from  $3\pi$ -exchange with single and double  $\Delta$ -excitation of either one nucleon.

rather lengthy formulas result from the multitude of spin-dependent terms in  $M_{3\pi\Delta\Delta}$  written in eq.(8). The imaginary parts of the isovector spin-spin and tensor NN-potentials  $\text{Im}W_{S,T}$  read:

$$\begin{aligned} \text{Im}W_S = & \frac{g_A^6 m_\pi^8}{(5\pi)^3 f_\pi^6 \Delta^4 (4u)^8} \int_2^{u-1} dw \sqrt{w^2 - 4} \lambda^{3/2}(w) \left\{ \frac{\lambda^2(w)}{42} + w^6 \left( \frac{26u^2}{9} + \frac{1}{21} \right) \right. \\ & + w^4 \left( \frac{2065u^4}{18} - \frac{1487u^2}{126} - \frac{1}{21} \right) + w^2 \left( \frac{779u^6}{18} - \frac{20519u^4}{42} + \frac{349u^2}{21} - \frac{2}{7} \right) \\ & + \frac{79u^8}{18} - \frac{243u^6}{14} + \frac{18545u^4}{42} - \frac{1633u^2}{126} + \frac{2}{3} + \frac{1}{63w^2} (556u^8 - 9358u^6 \\ & \left. + 12199u^4 + 556u^2 - 33) + \frac{1}{21w^4} (556u^8 - 1181u^6 + 697u^4 - 75u^2 + 3) \right\}, \quad (38) \end{aligned}$$

$$\begin{aligned} \text{Im}(\mu^2 W_T - W_S) = & \frac{g_A^6 m_\pi^8}{(5\pi)^3 f_\pi^6 \Delta^4 (4u)^8} \int_2^{u-1} dw \sqrt{(w^2 - 4)\lambda(w)} \left\{ \frac{\lambda^3(w)}{6} + \frac{w^{10}}{36} (403u^2 + 12) \right. \\ & + \frac{w^8}{9} (2494u^4 - 565u^2 - 9) - \frac{w^6}{18} (11707u^6 + 35060u^4 - 1993u^2 + 18) \\ & + \frac{w^4}{9} (3869u^8 + 29381u^6 + 42250u^4 - 423u^2 + 75) \\ & - w^2 \left( \frac{2629u^{10}}{36} + \frac{10670u^8}{9} + \frac{32977u^6}{6} + \frac{38701u^4}{9} + \frac{1997u^2}{36} + 15 \right) \\ & + 13 + \frac{u^2}{9} (47u^{10} - 716u^8 + 9501u^6 + 29894u^4 + 8791u^2 + 430) \\ & + \frac{1}{9w^2} (97u^{12} + 1920u^{10} - 2013u^8 - 2192u^6 + 2207u^4 + 32u^2 - 51) \\ & \left. + \frac{1}{3w^4} (97u^{12} - 400u^{10} + 633u^8 - 472u^6 + 163u^4 - 24u^2 + 3) \right\}. \quad (39) \end{aligned}$$

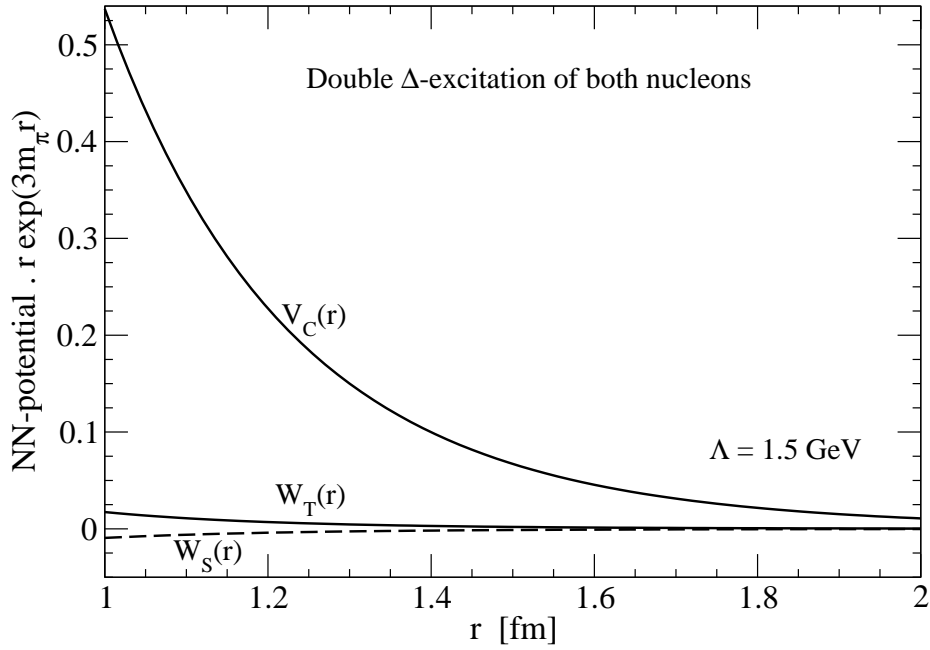


Figure 9: NN-potentials arising from  $3\pi$ -exchange with double  $\Delta$ -excitation of both nucleons.

The corresponding NN-potentials in  $r$ -space, multiplied with  $r \exp(3m_\pi r)$ , are shown in Fig. 9. The dominant feature is again a repulsive isoscalar central potential  $\tilde{V}_C(r)$ . It is however smaller than those encountered in the previous two subsections.

## 4 Conclusions

In this work we have studied the two-nucleon interaction which arises from the exchange of three pions and the excitation of  $\Delta(1232)$ -isobars in intermediate states. The pertinent two-loop spectral-functions have been calculated in the approximation of neglecting the energy-independence of the non-relativistic  $\Delta(1232)$ -propagator. A subsequent analysis of the NN-potentials in  $r$ -space has revealed that the main effect of these specific exchange and excitation mechanisms is isoscalar central repulsion. Other components, such as  $\tilde{W}_T(r)$  receive canceling contributions, or come out very small anyway. From the spectral-functions collected in section 3 one can reconstruct the NN-potentials in momentum-space via subtracted dispersion relations. This way one can include the interaction terms calculated in this work (in chiral effective field theory) into future fits to empirical NN phase shifts.

## References

- [1] E. Epelbaum, *Prog. Part. Nucl. Phys.* **57**, 654 (2006).
- [2] E. Epelbaum, H.W. Hammer and Ulf-G. Meißner, *Rev. Mod. Phys.* **81**, 1773 (2009).
- [3] R. Machleidt and D.R. Entem, *Phys. Rep.* **503**, 1 (2011).
- [4] E. Epelbaum and Ulf-G. Meißner, *Ann. Rev. Nucl. Part. Sci.* **62**, 159 (2012).
- [5] D.R. Entem, N. Kaiser, R. Machleidt and Y. Nosyk, *Phys. Rev.* **C91**, 014002 (2015).
- [6] E. Epelbaum, H. Krebs and Ulf-G. Meißner, arXiv, nucl-th/1412.0142; nucl-th/1412.4623.
- [7] N. Kaiser, S. Gerstendörfer and W. Weise, *Nucl. Phys.* **A637**, 395 (1998).
- [8] H. Krebs, E. Epelbaum and Ulf-G. Meißner, *Eur. Phys. J.* **A32**, 127 (2007).
- [9] E. Epelbaum, H. Krebs and Ulf-G. Meißner, *Phys. Rev.* **C77**, 034006 (2008).
- [10] N. Kaiser, *Phys. Rev.* **C62**, 024001 (2000).
- [11] N. Kaiser, *Phys. Rev.* **C63**, 044010 (2001).